SPATIO-TEMPORAL DYNAMICS AND INTERACTION OF LUMP SOLUTIONS FOR THE (4+1)-D FOKAS EQUATION

by

Hou-Ping DAI[a, b], Wei TAN[b*], and Zhou-Shun ZHENG[a]

[a] School of Mathematics and Statistics, Central South University, Changsha, China
[b] College of Mathematics and Statistics, Jishou University, Jishou, China

Original scientific paper
https://doi.org/10.2298/TSCI1804823D

The (4+1)-D Fokas equation is a new and important physical model. Its Hirota's bilinear form with a perturbation parameter is obtained by an appropriate transformation. A class of lump solutions and three different forms of spatio-temporal structure are obtained. Meanwhile, the theoretical analysis for the change of spatio-temporal structure is discussed by using the extreme value theory of multivariate function. Finally, the interaction between a stripe soliton and lump solution is discussed, and a new wave phenomenon that the lump solution is swallowed and drowned by the stripe soliton is investigated.

Key words: *(4+1)-D Fokas equation, Hirota's bilinear method, lump solution, spatio-temporal dynamics, interaction*

Introduction

It is well known that many phenomena arising in fluid mechanics and thermal science can be described by solitary waves [1-3]. The main tools in the open literature to treat the solitary waves are the exp-function method [4] and Hirota's bilinear method [5]. Several authors have contributed in this direction, in which Ma and He were the pioneers. Very recently, Ma and Zhou [6] applied the Hirota's bilinear method to obtain lump solutions of a class of quadratic functions. Meanwhile, the lump solutions and the interaction between lump solutions and other soliton solutions of many non-linear equations were studied [7-11]. However, the spatio-temporal pattern of solitary waves has been little treated though it becomes more and more important in thermal science and fluid mechanics as well. To illustrate the spatio-temporal property of a thermal problem, we consider a candle in the wind, which varies over space and time, local interactions in space can give rise to large scale spatio-temporal patterns, and *vice versa*. The principal goals to deal with such problems are statistics, machine learning, and others. In this paper spatio-temporal dynamics is used to study solitary waves to reveal their spatio-temporal properties.

Now, we consider the (4+1)-D Fokas equation:

$$u_{xt} - \frac{1}{4}u_{xxxy} + \frac{1}{4}u_{xyyy} + \frac{3}{2}(u^2)_{xy} - \frac{3}{2}u_{zw} = 0 \tag{1}$$

which is a generalization of the (2+1)-D KdV equation, Davey-Stewartson equation, and Kadomtsev-Petviashvili equation [12]. Here, by (x, y, z, t) are real (3+1)-D space and time, while

* Corresponding author, e-mail: tanwei1008@126.com; daihouping@163.com

w is a phenotype time to reveal effect of time interaction on the morphology of the solitary wave. Therefore, the (4+1)-D Fokas equation can also be called the (3+2)-D Fokas equation. Due to the important applications of spatio-temporal dynamics in practical problems, for example, in electrospinning process [13], bubble's shape change during the bubble electrospinning [14] and in thermal instability in the Taylor cone [15], it is necessary to study its analytical solution. To the best of our knowledge, there are many useful properties that have not been presented in the previous work. In this manuscript, we will study the lump solutions, spatio-temporal structure and interaction between a stripe soliton and lump solution of (4+1)-D Fokas equation by using Hirota's bilinear method. Finally, some new wave phenomena will be investigated and simulated by 3-D plots.

Spatio-temporal dynamics of lump solution

Lump solution and spatio-temporal structure

Firstly, the bilinear form of eq. (1) is obtained by taking the following transformation:

$$\xi = \alpha x + \beta y \tag{2}$$

and

$$u(\xi, z, \omega, \mathrm{t}) = u_0 + (\beta^2 - \alpha^2)(\ln f)_{\xi\xi} \tag{3}$$

where α and β are some wave parameter and $f(\xi, z, w, t)$ is an unknown real function, then taking $\alpha\beta \neq 0$ and $\alpha^2 \neq \beta^2$. Substituting eqs. (3) and (2) into eq. (1), a new bilinear equation which is different from the work [16] is obtained:

$$\text{Fokas}(f): \left[\mathrm{D}_\xi \mathrm{D}_t + \frac{1}{4}\beta(\beta^2 - \alpha^2)\mathrm{D}_\xi^4 + 3\beta u_0 \mathrm{D}_\xi^2 - \frac{3}{2\alpha}\mathrm{D}_{zw} \right] f\ f = 0 \tag{4}$$

where D is a bilinear operator [17].

In order to get a class of lump solutions of (4+1)-D Fokas equation, according to [6-9], we can assume that the solution has the following quadratic function form:

$$f(\xi, z, w, t) = a_0 + (a_1\xi + b_1 z + c_1 w + d_1 t + e_1)^2 + (a_2\xi + b_2 z + c_2 w + d_2 t + e_2)^2 \tag{5}$$

where a_0, a_i, b_i, c_i, d_i, and e_i, (i = 1, 2) are some real unknown constants to be determined. The following relations among the parameters can be obtained via inserting eq. (5) into eq. (4) with the help of MAPLE.

Case 1

$$a_0 = \frac{\alpha\beta a_2^4(\beta^2 - \alpha^2)}{2b_1c_1}, \quad d_1 = \frac{3(b_2c_1 + b_1c_2)}{2\alpha a_2}, \quad a_1 = 0, \quad d_2 = \frac{3(b_2c_2 - b_1c_1)}{2\alpha a_2} - 3\beta u_0 a_2 \tag{6}$$

where b_1c_1 and $a_2 \neq 0$ and a_2, b_1, b_2, c_1, c_2, e_1, and e_2 are some free real parameters. An exact lump solution is obtained by substituting eqs. (6) with eq. (5) into eq. (3):

$$u = u_0 + \frac{2a_2^2(\beta^2 - \alpha^2)\left[\alpha\beta\alpha_2^4(\beta^2 - \alpha^2)(2b_1c_1)^{-1} + \Theta^2 - \Delta^2\right]}{\left[\alpha\beta\alpha_2^4(\beta^2 - \alpha^2)(2b_1c_1)^{-1} + \Theta^2 + \Delta^2\right]^2} \tag{7}$$

where

$$\Theta = b_1 z + c_1 w + \frac{3(b_2 c_1 + b_1 c_2)}{2\alpha a_2} t + e_1$$

and

$$\Delta = a_2 \xi + b_2 z + c_2 w + \left[\frac{3(b_2 c_2 - b_1 c_1)}{2\alpha a_2} - 3\beta u_0 a_2 \right] t + e_2$$

The lump solution, eq. (7), contains some free parameters b_1, c_1, a_2, b_2, c_2, e_1, e_2, and u_0, which determined the diversity of spatio-temporal structure. Meanwhile, the asymptotic behavior of the lump solution can be found $u \to u_0$, either $\xi \to \pm\infty$ or $z \to \pm\infty$ or $w \to \pm\infty$ or $t \to \pm\infty$, it means that solution, eq. (7), has the characteristic of pulse solution. From fig. 1(a), we can clearly see that the lump solution has bright lump solution structure characteristics, which has one upward peak and two small downward projections, the main peak forms a much higher hill, the two downward projections are hidden under the plane wave [18]. However, the spatio-temporal structure of lump solution will vary with the change of the seven free parameter values. Figure 1(b) shows that the lump solution is a dark lump structure which contains one downward peak and two small upward projections. The 3-D image simulation indicates that when the values of these free parameters are changed, the spatio-temporal structure of eq. (7) is changed accordingly. Where, the curve drawn at the bottom of the figure is the contour line in figs. 1(a) and 1(b).

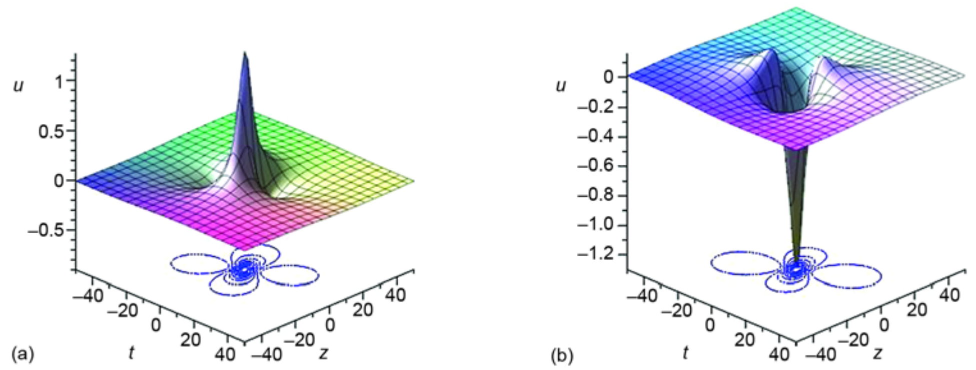

Figure 1. Spatio-temporal of the lump solution of eq. (7); $u_0 = 0$, $b_2 = 0{,}5$, $e_1 = e_2 = \xi = w = 0$, **(a)** $\alpha = 1$, $\beta = 3$, $a_2 = c_1 = 1$, $b_1 = 0.25$, $c_2 = 0.125$, **(b)** $\alpha = -3$, $\beta = 1$, $a_2 = 2$, $c_1 = 4$, $b_1 = 1$, $c_2 = 0.25$
(*for color image see journal web site*)

Case 2

$$a_0 = \frac{3\alpha\beta(\beta^2 - \alpha^2)\phi^2}{6 b_2 c_2 - 4\alpha a_2 \psi}, \quad b_1 = \frac{2\alpha\psi\phi - 3b_2\varphi}{3(a_1 c_2 - a_2 c_1)}, \quad d_2 = \frac{3\beta u_0 \sigma + 3(c_1^2 + c_2^2)(2\alpha)^{-1} - d_2\varphi}{a_2 c_1 - a_1 c_2} \tag{8}$$

where $\phi = a_1^2 + a_2^2, \varphi = a_1 c_1 + a_2 c_2, \psi = d_2 + 3\beta u_0 a_2, \sigma = a_1^2 c_2 - 2a_1 a_2 c_1 - a_2^2 c_2$, meanwhile, b_1 and d_2 needs to satisfy the conditions: $a_1 c_2 - a_2 c_1 \neq 0$. Substituting eqs. (8) with eq. (5) into eq. (3), we get a new lump solution:

$$u = u_0 + 2(\beta^2 - \alpha^2)\frac{\phi\left[\dfrac{3\alpha\beta(\beta^2-\alpha^2)\phi^2}{6bc - 4\alpha a_2\psi} + \Theta^2 + \Delta^2\right] - 2(a_1\Theta + a_2\Delta)^2}{\left[\dfrac{3\alpha\beta(\beta^2-\alpha^2)\phi^2}{6bc - 4\alpha a_2\psi} + \Theta^2 + \Delta^2\right]^2} \tag{9}$$

where $\Theta = a_1\xi + b_1z + c_1w + d_1t + e_1$ and $\Delta = a_2\xi + b_2z + c_2w + d_2t + e_2$. Bright lump structure and dark lump structure are obtained by selecting different parameter values. Meanwhile, we noticed that the conditions $a_1c_2 - a_2c_1 \neq 0$, which means that the two directions (a_1, c_1), and (a_2, c_2) in the ξw-plane are not parallel, therefore, the space structure of lump solutions in ξw-plane has the characteristics of kinky wave (see fig. 2).

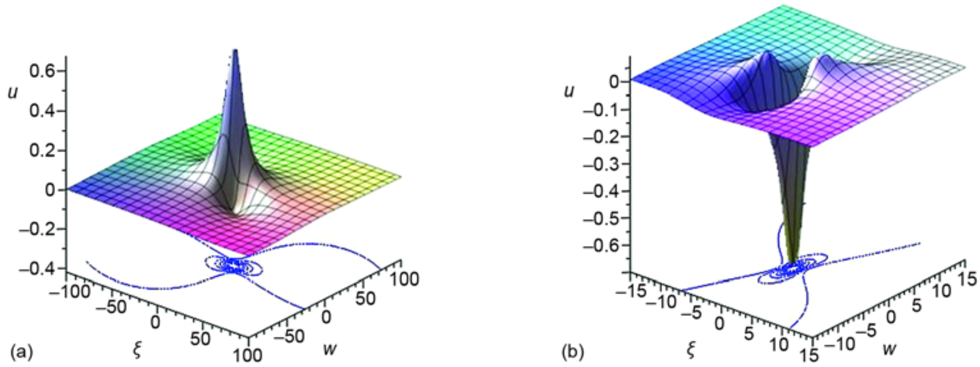

Figure 2. Space structure of the lump solution of eq. (9); $a_2 = 1$, $b_2 = d_2 = 2$, $c_1 = 0.5$, $c_2 = 4$, $e_1 = e_2 = z = t = 0$, $u_0 = 0$, (a) $\alpha = 1$, $\beta = 3$, $a_1 = 3$, (b) $\alpha = -3$, $\beta = 1$, $a_1 = 4$ (*for color image see journal web site*)

Case 3

$$u_0 = 0, \quad a_0 = \frac{3\phi^2\beta(\alpha^2-\beta^2)}{4a_2d_2}, \quad c_2 = 0, \quad b_1 = -\frac{2\alpha a_2 d_2}{3c_1},$$
$$b_2 = \frac{2\alpha a_1 d_2}{3c_1}, \quad d_1 = 0, \quad e_2 = 0 \tag{10}$$

where $\phi = a_1^2 + a_2^2, a_1, c_1, e_1, a_2$ and d_2, are some free real numbers. A new lump solution is obtained by substituting eqs. (10) with eq. (5) into eq. (3):

$$u(\xi,z,w,t) = 2(\beta^2-\alpha^2)\frac{\left[\dfrac{3\phi^2\beta(\alpha^2-\beta^2)}{4a_2d_2} + \Theta^2 + \Delta^2\right] - 2(a_1\Theta + a_2\Delta)^2}{\left[\dfrac{3\phi^2\beta(\alpha^2-\beta^2)}{4a_2d_2} + \Theta^2 + \Delta^2\right]^2} \tag{11}$$

where $\Theta = a_1\xi - 2\alpha a_2d_2(3c_1)^{-1}z + c_1w + e_1$ and $\Delta = a_2\xi + 2\alpha a_1d_2(3c_1)^{-1}z + d_2t$. The solution of eq. (11) have similar characteristics and space structure with solution of eq. (7). The features of the bright and dark lump structures are reflected by changing the values of these free parameters α, β, a_1, c_1, e_1, a_2 and d_2.

Theoretical analysis for the spatio-temporal structure changes

In this section, we will provide a theoretical analysis of the spatio-temporal structure changes of lump solutions of eqs. (7), (9), and (11). Here, we mainly discuss two cases of $u_0 = 0$ and $u_0 \neq 0$.

When $u_0 \neq 0$, we focus on the exact lump solution of eq. (7) by the perspective of the extreme value theory of two element function. Here, we consider the case of $\xi = 0$, $w = 0$, in other words, considering the critical point of the function $U(z, t) = u(0, z, 0, t)$. In order to obtain the extremum values of the function $U(z, t)$, it is needed to calculate the necessary condition:

$$\begin{cases} \dfrac{\partial}{\partial z} U(z,t) = 0 \\ \dfrac{\partial}{\partial t} U(z,t) = 0 \end{cases} \tag{12}$$

Thus, solving condition of eq. (12) leads to a critical point $p(z, t)$, where:

$$\begin{cases} z = -\dfrac{\left(b_1c_2 + b_2c_1\right)e_2 + \left(b_1c_1 - b_2c_2 + 2\beta u_0 \alpha a_2^2\right)e_1}{\Omega} \\ t = \dfrac{2\alpha a_2\left(b_1e_2 - b_2e_1\right)}{3\Omega} \end{cases} \tag{13}$$

where $\Omega = c_1b_1^2 + c_1b_2^2 + 2b_1\alpha\beta u_0 a_2^2 \neq 0$. Substituting eq. (13) into two element function $U(z, t)$, through complicated calculation, we can get the extreme value:

$$U(y,t)\big|_p = u_0 + \frac{4b_1c_1}{\alpha\beta a_2^2} \tag{14}$$

Furthermore, at the point p, the second order derivative can be obtained:

$$\begin{cases} A = \dfrac{\partial^2 U(z,t)}{\partial z^2} = \dfrac{16b_1^2c_1^2\left(b_1^2 + 3b_2^2\right)}{\alpha^2\beta^2a_2^6\left(\alpha^2 - \beta^2\right)} \\ H\left(U\right) = \begin{vmatrix} \dfrac{\partial^2 U(z,t)}{\partial z^2} & \dfrac{\partial^2 U(z,t)}{\partial z \partial t} \\ \dfrac{\partial^2 U(z,t)}{\partial t \partial z} & \dfrac{\partial^2 U(z,t)}{\partial t^2} \end{vmatrix}_p = \dfrac{1728b_1^4c_1^4\Omega^2}{\beta^4\alpha^6a_2^{14}\left(\alpha^2 - \beta^2\right)} \end{cases} \tag{15}$$

By using the discriminant theory of extremum points for the two-variables function, meanwhile, notice that $b_1c_1\Omega \neq 0$ in eqs. (15), we can have the following results:

(1) if $\alpha^2 < \beta^2$, this is, $A < 0$ and $H(U) > 0$, the p is a maximum point, $u(\xi, z, w, t)$ shows bright lump structure characteristics (fig. 1a).
(2) if $\alpha^2 > \beta^2$, this is, $A > 0$ and $H(U) > 0$, the p is a minimum point, $u(\xi, z, w, t)$ shows dark lump structure characteristics (see fig. 1b).

When $u_0 = 0$, we mainly discuss the *Case 3*. let $U(\xi, z) = u(\xi, z, 0, 0)$ in eq. (11). After calculating, the point $p[-(a_1e_1)/a\phi, -(3a_2c_1e_1)/(a\alpha d2\phi)]$ is a critical point of the function $U(\xi, z)$, and:

$$U(\xi,z)\big|_p = -\frac{8}{3}\frac{a_2 d_2}{\phi\beta} \tag{16}$$

Thus, at the point p, the second order derivative can be obtained:

$$\begin{cases} B = \dfrac{\partial^2 U(\xi,z)}{\partial \xi^2} = \dfrac{64}{3}\dfrac{a_2^2 d_2^2}{\beta^2\left(a_1^2+a_2^2\right)^2\left(\alpha^2-\beta^2\right)} \\ H(U) = \begin{vmatrix} \dfrac{\partial^2 U(\xi,z)}{\partial \xi^2} & \dfrac{\partial^2 U(\xi,z)}{\partial \xi \partial z} \\ \dfrac{\partial^2 U(\xi,z)}{\partial z \partial \xi} & \dfrac{\partial^2 U(\xi,z)}{\partial z^2} \end{vmatrix}_p = \dfrac{16384}{243}\dfrac{a_2^2 d_2^6 \alpha^2}{\beta^4 c_1^2\left(a_1^2+a_2^2\right)^6\left(\alpha^2-\beta^2\right)^2} \end{cases} \tag{17}$$

However, through the extreme value discrimination theory of two element function, we can the following results:

(1) if $\alpha^2 < \beta^2$, this is, $B < 0$ and $H(U) > 0$, the p is a maximum point, u shows bright lump structure characteristics.

(2) if $\alpha^2 > \beta^2$, this is, $B > 0$ and $H(U) > 0$, the p is a minimum point, u shows dark lump structure characteristics.

From the previous extreme value theory analysis and 3-D graphic simulation, we can know that the change of spatio-temporal structure mainly depends on the value of parameters α and β, and is not directly related to the perturbation parameter u_0. So, there will be a bright lump structure, when $\alpha^2 < \beta^2$; the dark lump structure appears, when $\alpha^2 > \beta^2$. When $\alpha\beta \neq 0$ and $\alpha^2 \neq \beta^2$, the bilinear form eq. (4) does not exist, we do not go deep research here, some related results can be viewed in [15].

Interaction

Here, we construct the interaction between a stripe soliton and lump solution for the (4+1)-D Fokas equation. To obtain the interaction between stripe soliton and lump solution, add an exponential function on the basis of the quadratic function eq. (5), that is:

$$f = a_0 + (a_1\xi + a_2 z + a_3 w + a_4 t + a_5)^2 + (a_6\xi + a_7 z + a_8 w + a_9 t + a_{10})^2 + \sigma e^{a_{11}\xi + a_{12}z + a_{13}w + a_{14}t + a_{15}} \tag{18}$$

Substituting eq. (18) into eq. (4) with eq. (3), through the tedious and long calculation, we can get the following cases:

Case 1

$$\begin{cases} a_0 = \dfrac{a_3^2}{a_{13}^2},\ a_1 = \dfrac{a_3 a_{11}}{a_{13}},\ a_2 = \dfrac{a_3 a_{11}\left(\Theta a_{13}^2 + \Delta a_{11} + a_{14}\right)}{a_{13}^2},\ a_3 = a_3,\ a_4 = \dfrac{a_3\left(a_{14} - 2\Theta a_{11}^2\right)a_{11}}{a_{13}} \\ a_5 = a_5, a_6 = 0,\ a_7 = \dfrac{2\alpha\Theta a_{11}^4 a_3^2}{a_8 a_{13}^2},\ a_8 = a_8,\ a_9 = \dfrac{3\Theta a_3^2 a_{11}^3 + \Theta a_8^2 a_{11}^2 + a_8^2 a_{14}}{a_{13}},\ a_{10} = a_{10} \\ a_{11} = a_{11},\ a_{12} = \dfrac{a_{11}\left(\Theta a_{13}^2 + \Delta a_{11} + a_{14}\right)}{a_{13}}, a_{13} = a_{13}, a_{14} = a_{14},\ a_{15} = a_{15} \end{cases} \tag{19}$$

Case 2

$$\begin{cases} a_0 = \dfrac{a_3^2}{a_{13}^2},\ a_1 = \dfrac{a_3 a_{11}}{a_{13}},\ a_2 = \dfrac{a_3 a_{11}(\Theta a_{13}^2 + \Delta a_{11} + a_{14})}{a_{13}^2},\ \ a_3 = a_3,\ a_4 = \dfrac{a_3(a_{14} - 2\Theta a_{11}^2)a_{11}}{a_{13}} \\ a_5 = a_5, a_6 = 0,\ a_7 = \dfrac{2\alpha\Theta a_{11}^4 a_3^2}{a_8 a_{13}^2},\ \ a_8 = a_8,\ a_9 = \dfrac{3\Theta a_3^2 a_{11}^3 + \Theta a_8^2 a_{11}^2 + a_8^2 a_{14}}{a_{13}},\ a_{10} = a_{10} \\ a_{11} = a_{11},\ a_{12} = \dfrac{a_{11}(\Theta a_{13}^2 + \Delta a_{11} + a_{14})}{a_{13}}, a_{13} = a_{13}, a_{14} = a_{14},\ a_{15} = a_{15} \end{cases} \tag{20}$$

where $\Theta = 0.25\beta(\beta^2 - \alpha^2)$ and $\Delta = 3\beta u_0$ in *Case 1* and *Case 2*. So, substituting eqs. (19) (or eqs. (20)) with eq. (18) into eq. (3), we can obtain a mixed type algebraic-exponential solitary wave solutions of (4+1)-D Fokas equation:

$$u(\xi, z, w, t) = u_0 + \left(\beta^2 - \alpha^2\right)\frac{2\left(a_1^2 + a_6^2\right) + \delta a_{11}^2 l}{a_0 + m^2 + n^2 + \delta l} - \frac{\left(2ma_1 + 2na_6 + a_{11}\delta l\right)^2}{\left(a_0 + m^2 + n^2 + \delta l\right)^2} \tag{21}$$

where $m = a_1\xi + a_2 z + a_3 w + a_4 t + a_5$, $n = a_6\xi + a_7 z + a_8 w + a_9 t + a_{11}$ and $l = e^{a_{11}\xi + a_{12}z + a_{13}w + a_{14}t + a_{15}}$. In order to simulate the 3-D graph of the interaction between the lump solution and the stripe soliton, we take the parameter $u_0 = a_5 = a_{10} = a_{15} = w = 0$, $\alpha = 1$, $\beta = 2$, $a_3 = 4$, $a_8 = 1$, $a_{11} = -1$, $a_{13} = -12$, $a_{14} = 0.5$, and $\beta = 1$ in *Case 1*.

From fig. 3, we can clearly observe soliton fusion phenomenon. Figure 3(a) shows the solution u consists of a stripe soliton and a lump soliton at time $t = -2$. With the development of time, t, the lump soliton is drowned or swallowed up by stripe soliton in the process of the interaction of two solitons. When $t = 0$, the lump soliton starts to be swallowed by the stripe soliton. This reflects the completely non-elastic interaction between two solitary waves.

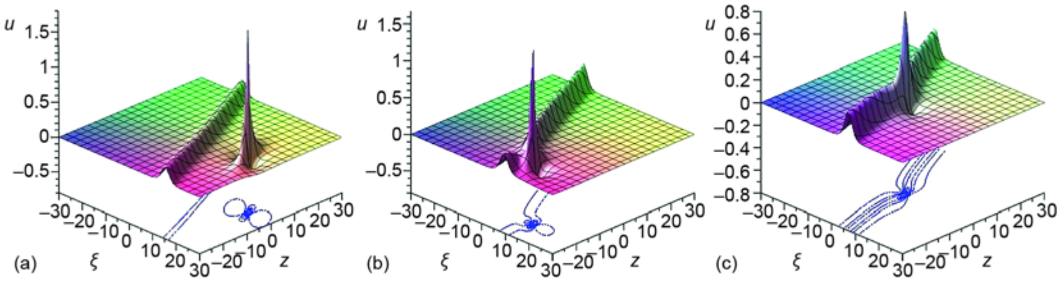

Figure 3. Plots of interactions at different times; (a) *t* = –2, (b) *t* = –1, (c) *t* = 0
(*for color image see journal web site*)

Conclusions

In this work, the (4+1)-D Fokas equation is reduced to the (3+1)-D non-linear partial derivative (NLPD) by an appropriate transformations eq. (2). The bilinear form with a small perturbation parameter and some exact lump solutions of (4+1)-D Fokas equation are obtained by Hirota's bilinear method and a special class of quadratic function. The dark lump structure, bright lump structure and kinky lump structure in different variables are simulated by taking different parameter values, these results reflect the diversity of spatio-temporal property of lump solution. Additionally, on the basis of different structures of these lump solutions, we analyze the theoretical reason, mainly the size of the α^2 and β^2 determined to understand the structural feature. Finally, the interaction between the stripe soliton and lump solution is studied, the fusion phenomenon of solitons is simulated by 3-D plots. As far as we know, these novel properties and interesting spatio-temporal dynamics are investigated for the first time in (4+1)-D Fokas equation. Our results enrich the variety of the dynamics characteristics of fluid mechanics and thermal science.

Acknowledgment

The work was supported by the National Key Research and Development Program of China (Grant No. 2017YFB0701700), Educational Commission of Hunan Province of China (Grant No. 16c1307, 17C1297), and Jishou University Natural Science Foundation (Grant No. Jd1801).

References

[1] He, J.-H., Li, Z. B., Converting Fractional Differential Equations into Partial Differential Equations, *Thermal Science, 16* (2012), 2, pp. 331-334
[2] Craik, A. D. D., Adam, J. A., Evolution in Space and Time of Resonant Wave Triads. I. The 'Pump-Wave Approximation', *Proceedings of the Royal Society A, 363* (1978), 1713, pp. 243-255
[3] Tan, W., *et al.,* Dynamical Analysis of Lump Solution for the (2+1)-Dimensional ITO Equation, *Thermal Science, 21* (2017), 4, pp. 1673-1679
[4] He, J.-H., Exp-Function Method for Fractional Differential Equations. *International Journal of Nonlinear Sciences & Numerical Simulation, 14* (2013), 6, pp. 363-366
[5] Hirota, R., Exact Solution of the Korteweg-de Vries Equation for Multiple Collisions of Solitons, *Physical Review Letters, 27* (1971), 18, pp. 1192-1194
[6] Ma, W. X., Zhou. Y., Lump Solutions to Nonlinear Partial Differential Equations via Hirota Bilinear Forms, *International Journal of Modern Physics B, 30* (2016), 28, 1640018
[7] Tan, W., Dai. Z. D., Spatiotemporal Dynamics of Lump Solution to the (1+1)-Dimensional Benjamin-Ono Equation, *Nonlinear Dynamics, 89* (2017), 4, pp. 2723-2728
[8] Ma, W. X., Lump Solutions to the Kadomtsev-Petviashvili Equation, *Physics Letters A, 379* (2015), 36, pp. 197-198
[9] Wang, C. J, Spatiotemporal Deformation of Lump Solution to (2+1)-Dimensional KdV Equation, *Nonlinear Dynamics, 84* (2015), 2, pp. 697-702
[10] Tan, W., Dai. Z. D., Dynamics of Kinky Wave for (3+1)-Dimensional Potential Yu-Toda-Sasa-Fukuyama Equation, *Nonlinear Dynamics, 85* (2016), 2, pp. 817-823
[11] Tan, W., *et al.* Emergence and Space-Time Structure of Lump Solution to the (2+ 1)-Dimensional Generalized KP Equation, *Pramana, 89* (2017), 5, pp. 77-84
[12] Fokas, A. S., Integrable Nonlinear Evolution Partial Differential Equations in 4+2 and 3+1 Dimensions. *Physical Review Letters, 96* (2006), 19, pp. 190-201
[13] Doshi, J., Reneker, D. H., Electrospinning Process and Application of Electrospun Fibers, *Journal of Electrostatics, 35* (1995), 2, pp. 151-160
[14] Faraz, N., *et al.,* A Simple Mathematical Model for Prediction of Fibre Size in the Bubble Electrospinning. *Journal of Computational & Theoretical Nanoscience, 10* (2012), 1, pp. 664-665
[15] Parrish, I. J., Stone, J. M., Nonlinear Evolution of the Magnetothermal Instability in Two Dimensions, *Astrophysical Journal, 633* (2005), 1, pp. 334-348
[16] Zhang S., *et al.,* Bilinearization and New Multisoliton Solutions for the (4+1)-Dimensional Fokas Equation, *Pramana-J. Phys. 86* (2016), 6, pp. 1259-1267
[17] Dai, Z. D., *et al.,* The Three-Wave Method for Nonlinear Evolution Equations, *Nonlinear Science Letters A, 1* (2010), 1, pp. 77-82
[18] Wang, C. J., *et al.,* Interaction Between Kink Solitary Wave and Rogue Wave for (2+1)-Dimensional Burgers Equation, *Mediterranean Journal of Mathematics, 13* (2016), 3, pp. 1087-1098

Paper submitted: September 2, 2017
Paper revised: September 27, 2017
Paper accepted: December 15, 2017